Supporting Information

Carbon-bridged (*p*-phenylenevinylene) polymer for high-performance solution-processed distributed feedback lasers

Marta Morales-Vidal, José A. Quintana, José M. Villalvilla, Pedro G. Boj, Hiroki Nishioka, Hayato Tsuji, Eiichi Nakamura, Guy L. Whitworth, Graham A. Turnbull, Ifor D. W. Samuel and María A. Díaz-García

Dr. M. Morales-Vidal,[+] Dr. J. M. Villalvilla, Prof. M. A. Díaz-García
Dpto. Física Aplicada, Instituto Universitario de Materiales de Alicante (IUMA) and Unidad Asociada UA-CSIC
Universidad de Alicante
Alicante 03080, Spain
E-mail: maria.diaz@ua.es

Dr. J. A. Quintana, Dr. P. G. Boj
Dpto. Óptica, IUMA and Unidad Asociada UA-CSIC
Universidad de Alicante
Alicante 03080, Spain

H. Nishioka, Prof. H. Tsuji,[++] Prof. E. Nakamura
Department of Chemistry, School of Science
The University of Tokyo
Hongo, Bunkyo-ku, Tokyo 113-0033, Japan

Dr. G. L. Whitworth, Prof. G. A. Turnbull, Prof. I. D. W. Samuel
Organic Semiconductor Centre, SUPA, School of Physics and Astronomy
University of St Andrews
St Andrews, KY16 9SS, United Kingdom

[+] Present address: Grupo de Investigación en Aplicaciones del Láser y Fotónica, Dpto. Física Aplicada, University of Salamanca, Salamanca, E-37008, Spain
[++] Present address: Department of Chemistry, Faculty of Science, Kanagawa University, 2946 Tsuchiya, Hiratsuka 259-1293, Japan

S1. Comparison of absorption and emission spectra in solution and thin-film

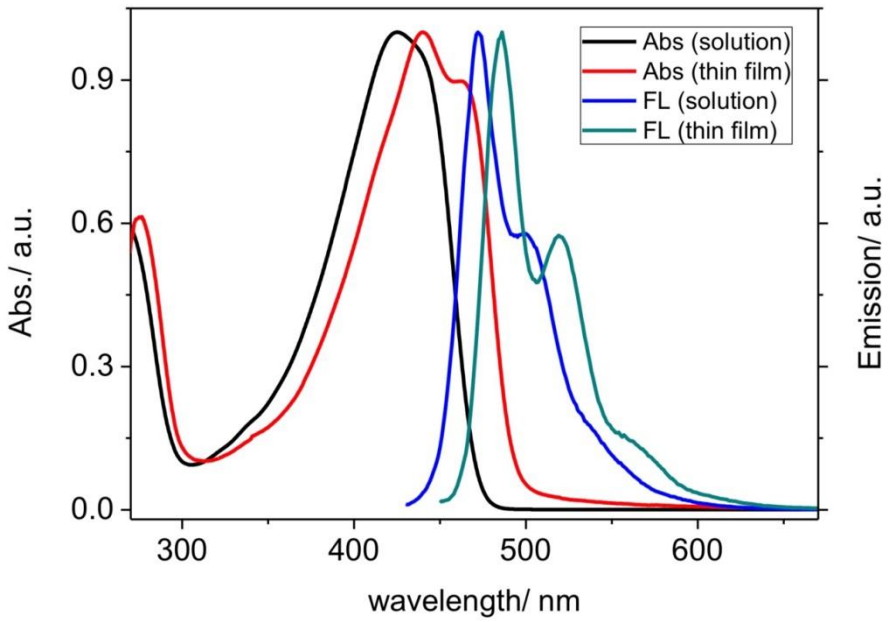

Figure S1: Absorption and emission spectra of poly-COPV1 in solution or thin-film. Spectra in solution were obtained using chloroform solutions with concentrations of 3 mg/L (absorption) and 0.3 mg/L (emission).

S2. Ellipsometry measurements

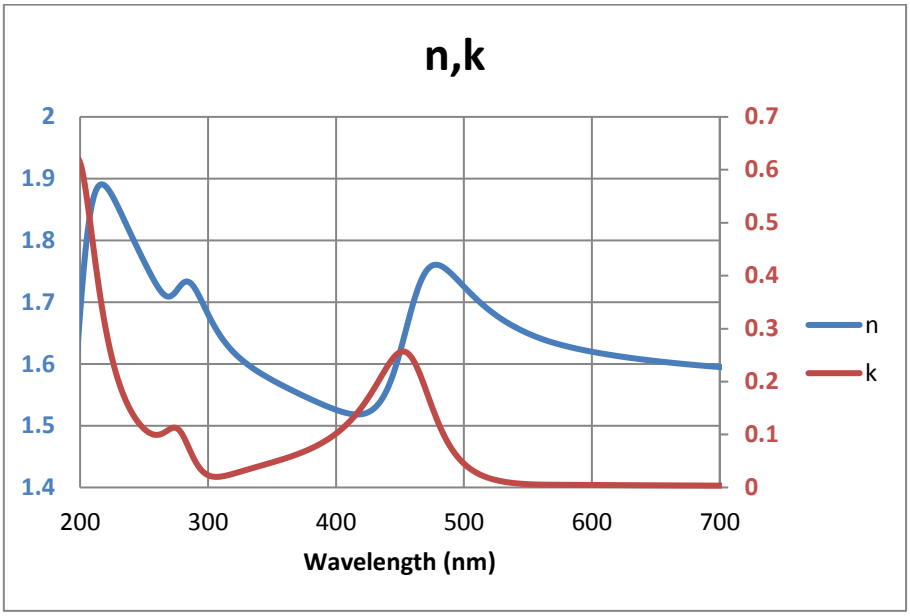

Figure S2: Refractive index (*n*) and extinction coefficient (*k*) of neat film of poly-COPV1 (thickness of 42 nm), determined by means of variable angle spectroscopic ellipsometry measurements using a J. A. Woollam Co.Inc.M2000-DI ellipsometer.

S3. Quinoidal resonance structure and molecular orbitals

(a)

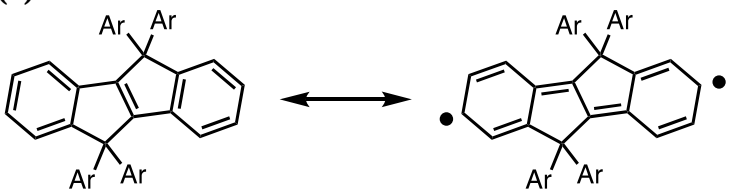

(b)

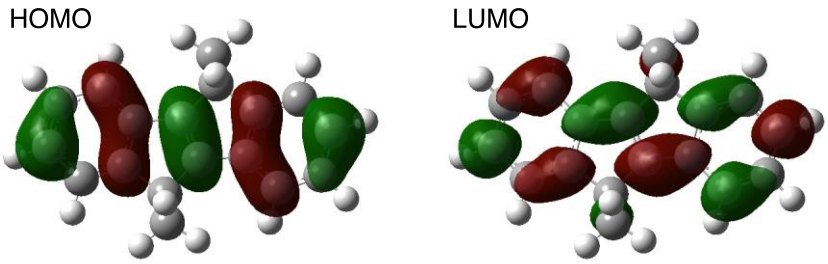

(c)

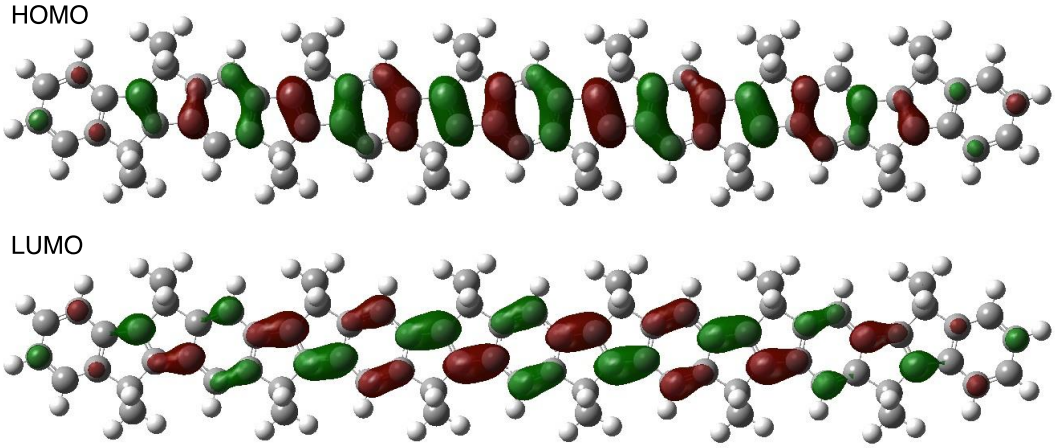

Figure S3: (a) Quinoidal resonance structure of COPV1; (b) HOMO (π) and LUMO (π*) of COPV1; (c) HOMO (π) and LUMO (π*) of COPV6.

S4: ASE Variable Stripe Length study for determination of net gain coefficient

When ASE is the mechanism responsible for the observation of spectral gain narrowing and of a sudden increase of the output intensity at a given pump intensity (the ASE threshold), the output intensity at the end of the stripe should follow the expression:

$$I(\lambda) = \frac{A(\lambda)I_p}{g(\lambda)}\left(e^{g(\lambda)l} - 1\right) \qquad \text{(Eq. 1)}$$

where A (λ) is a constant related to the cross section for spontaneous emission, I_p is the pump intensity, g (l) is the net gain coefficient and l is the length of the pump stripe. Note that this expression does not take into account saturation effects appearing at thigh pump intensities.

The net gain coefficient for a given pump intensity can be determined by fitting the output intensity at the peak of the emission spectrum as a function of the pump stripe length.

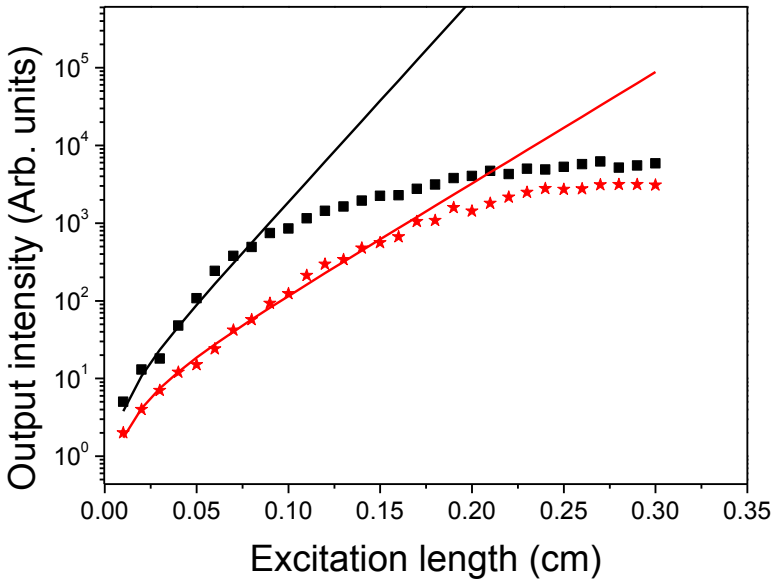

Figure S4. Emission intensity at the wavelength at which ASE appears (λ = 527 nm) versus the length of the excitation stripe for a neat film of poly-COPV1 at pump intensities of 34.8 and 18.2 kW cm^{-2} (squares and starts respectively). The solid lines are fits to the data using Supplementary Equation 1, from which net gain coefficients, g, of 60 cm^{-1}and 33 cm^{-1}, respectively, were obtained. Note that for very long excitation lengths gain saturation is present, so only points obtained at short excitation lengths were used for the fit.

S5: Poly-COPV1 DFB lasers with substructured gratings.

Table S1. Geometrical and performance parameters of various poly-COPV1 DFB lasers with Type 2: R_{Bel}^{S} architecture. In all cases the substrate is glass, the resonator material is the mr-XNIL26 UV-NIL resist and the period of the grating unit cell is 350 nm.

Device Label [a]	h [b] **(nm)**	Λ [c] **(nm)**	**Stamp**	W [d] **(nm)**	X [e] **(nm)**	λ_{pump} [f] **(nm)**	λ_{DFB} [g] **(nm)**	$I_{th\text{-}DFB}$ [h] **(kW/cm^2)**	**FWHM** [i] **(nm)**
2	≈140	350	A	95	75	445	534.9	0.7	< 0.5
2b	≈140	350	C	60	105	445	532.7	1.3	< 0.5
2c	<250	350	A	95	75	450	542.8	1.2	< 0.5
2d	<250	350	B	100	60	450	542.4	2.0	1.0
2e	<250	350	C	60	105	450	542.2	1.0	<0.5

[a] Number on the label refers to the device Type; [b] Film thickness (error is ± 5 nm); [c] Grating period; [d] Width of the two ridges within the unit cell of a substructured grating; [e] Separation between the two ridges within the unit cell of a substructured grating; [f] Pump wavelength; [g] DFB wavelength (error is ± 0.2 nm); [h] DFB threshold (error ~ 10%, estimated statistically as the standard deviation from measurements on several nominally identical samples); [i] DFB linewidth, defined as the full width at half of the maximum (error is ±0.5).

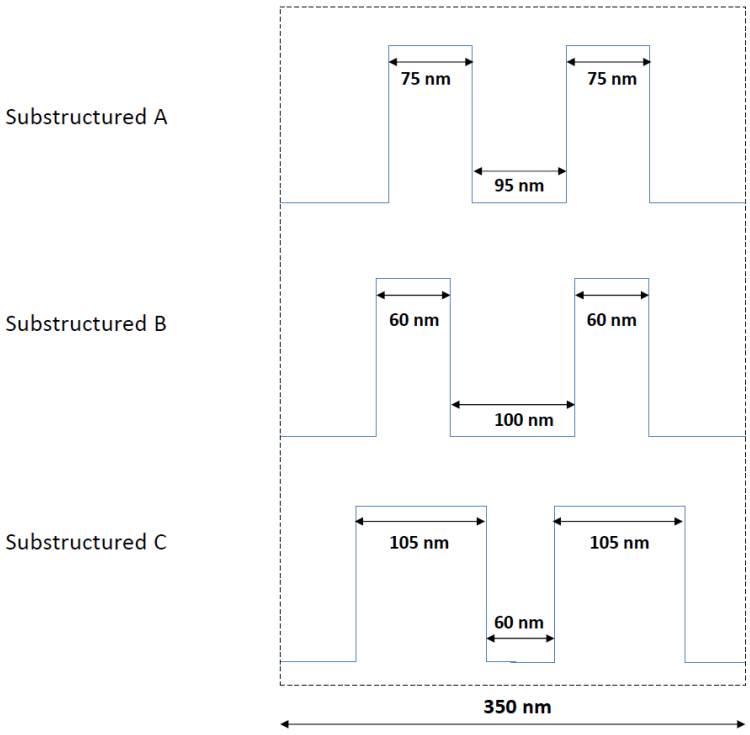

Figure S5. Scheme of the stamp structure used to imprint the substructured gratings indicated in Table S1.